Click Here for Full Article

Aspect-related microclimatic influences on slope forms and processes, northeastern Arizona

Benjamin N. Burnett,[1] Grant A. Meyer,[1] and Leslie D. McFadden[1]

[1] Climate is a major control on geomorphology, yet the effects of aspect-related differences in microclimate have been little studied. We examined several 60–100-m-deep canyons in semiarid northeastern Arizona, where rock type and structure are essentially constant, but where field data and a high-resolution digital elevation model reveal consistent morphologic and microclimatic differences between asymmetric north- and south-facing sideslopes. Cliffs account for 29% of the vertical relief of south-facing slopes but only 2.5% of north-facing slopes. Excluding cliffs, south-facing slopes are 1–3° steeper than north-facing slopes and have significantly less weathered bedrock. We monitored air, surface and subsurface temperatures and soil moisture at 0.5-h intervals at four locations over 1 year. South-facing slopes were 1.4–5.6°C warmer and soil moisture tension at 10-cm-depth averages at least 78 kPa lower (drier) than on north-facing slopes. The dominant rock type in the study area, Morrison formation sandstone, weathers primarily by clay hydration. These sandstones form disaggregated mantles where weathering exceeds erosion but also maintain steep slopes and cliffs where little weathered. South-facing slopes were too dry during most of the instrumented year for significant clay expansion, whereas the north-facing bedrock slope was moist all year. Cliff growth thus occurs preferentially on warmer and drier slopes, where weathering is reduced. Small north-facing cliffs (typically <3 m) could have formed during the Holocene but cliffs up to 70 m high on southerly aspects require more time to form and likely persisted or expanded under cooler and wetter late Pleistocene climates.

Citation: Burnett, B. N., G. A. Meyer, and L. D. McFadden (2008), Aspect-related microclimatic influences on slope forms and processes, northeastern Arizona, *J. Geophys. Res.*, *113*, F03002, doi:10.1029/2007JF000789.

1. Introduction

[2] Understanding climatic controls on geomorphic processes is a fundamental goal of geomorphology, one that has been addressed using a variety of field and modeling approaches. Relatively few studies, however, have taken advantage of the contrasting microclimate between slopes of different aspect, termed topoclimate by *Thornthwaite* [1961], to investigate climate-related differences in processes and landforms [e.g., *Melton*, 1960; *Churchill*, 1981, 1982; *Branson and Shown*, 1989; *Kirkby et al.*, 1990]. Because rock type, base level control, and other influences can be held essentially constant, topoclimate provides a powerful tool for understanding the geomorphic effects of persistent climatic differences on otherwise similar slopes. Previous work shows that topoclimatic contrasts may produce asymmetric valley morphology through control of slope weathering, erosional, and depositional processes. These slope processes are also a function of local geologic, vegetative, and environmental controls, and slope evolution has occurred over long timescales

subject to Quaternary climate change. Thus, although the influence of aspect is often apparent, valley asymmetry can have complex and disparate origins, as evident in reviews by *Wilson* [1968], *Kennedy* [1976], *Dohrenwend* [1978], and *Naylor and Gabet* [2007]. We apply a topoclimatic approach to three small (∼0.5 km²) canyons east of the small town of Blue Gap, northeastern Arizona, where a strong asymmetry is apparent: south-facing slopes are steeper than north-facing slopes, and have more cliff area and exposed bedrock (Figures 1 and 2).

[3] Sandstones of the Morrison formation dominate the canyon sides in this area and form south-facing cliffs over 70 m high, but the same sandstone units underlie moderate slopes that dominate northerly aspects (Figure 1). We hypothesize that these contrasts in geomorphic expression result from aspect-related differences in insolation that influence temperature, evapotranspiration and ultimately moisture availability for bedrock weathering. Highly weatherable bedrock has been shown to exhibit large geomorphic responses to minor climate fluctuations in semiarid regions, especially in rocks with moisture sensitive minerals or cements [*Bull*, 1991; *McFadden and McAuliffe*, 1997]. In addition, steep topography combines with intense solar radiation in the clear, dry air and high altitude of northeastern Arizona to produce large differences in effective insolation and topoclimate on different slope aspects. We

[1]Department of Earth and Planetary Sciences, University of New Mexico, Albuquerque, New Mexico, USA.
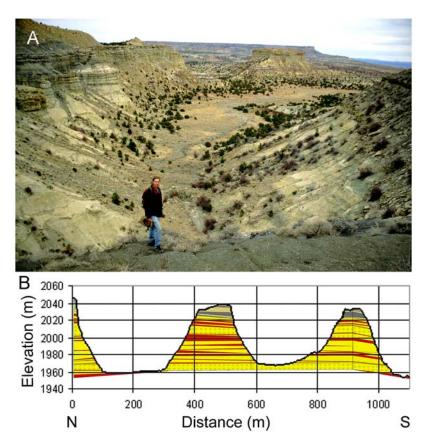
Figure 1. (a) Canyon asymmetry illustrated in a view looking east from the canyon rim at the head of basin 4. (b) N-S topographic profile across the study canyons showing stratigraphy (sandstones are light patterned whereas shales are dark patterned). The Dakota formation comprises about the top 10 m on each ridge crest. Profile location shown in Figure 2.

measured temperature, soil moisture, and slope characteristics to link topoclimate to hillslope processes and resulting geomorphology. The effects of topoclimate on slope processes and forms are inferred from four main types of measurements: (1) characteristics of slope facets measured in the field; (2) slope and cliff properties calculated from a digital elevation model (DEM); (3) stratigraphy and petrography of differentially weathered sandstones; and (4) modeled insolation and measured near-surface temperature and soil moisture on north- and south-facing slopes.

2. Study Area

[4] The study area lies in the southern Colorado plateau, along the eastern Black Mesa escarpment in northeastern Arizona (Figure 2). Basins informally designated 1 through 5 are canyons cut into the escarpment. Stepped pediment remnants indicate episodic canyon cutting within the late Quaternary [*Tillery et al.*, 2003]. All five drainages are well graded to the same master stream, thus slope evolution was affected equally by base level control in each basin. Minor net aggradation of valley floors occurred in the late Holocene, as discussed by *Tillery et al.* [2003], who studied basins 1–3. We focus on basins 3, 4, and 5, which drain eastward and have predominantly north- and south-facing sideslopes with about 100 m of relief. Asymmetry of the sideslopes is unlikely to be a function of differential

undercutting by axial streams [cf. *Melton*, 1960; *Dohrenwend*, 1978], as the valley floors are mostly broad, flat alluvial fill surfaces and there is no evidence for systematic lateral displacement of the channel by sideslope sediment inputs (Figures 1 and 2). Except in some steep, narrow canyon heads, toeslope colluvial wedges are thin and do not impinge on the channel, and small, low-gradient fans built by some sideslope drainages are mostly sandy, with limited potential to displace the axial channel. Active tectonic tilting causing preferential channel migration is also highly improbable, as there is no evidence for local-scale Quaternary deformation in this part of the Colorado Plateau [*Graf et al.*, 1987]. Therefore, valley asymmetry in the study area can be assessed in light of aspect-influenced hillslope processes, without complications arising from differential lateral erosion of footslopes [*Churchill*, 1981].

[5] Most parts of the study area canyons are cut into the weakly cemented sandstones and mudstones of the Jurassic Morrison formation and overlying sandstones and shales of the Cretaceous Dakota formation. Relatively resistant, silica-cemented Dakota sandstones are of variable thickness and form a caprock where the weak overlying Mancos Shale has been stripped away, or a ledge with a distinct break in slope angle. This study focuses on the canyon sideslopes, which extend from this break in slope to the relatively flat alluvial floor. Above the upper ends of the canyons, slopes descending from the high Toadindaaska
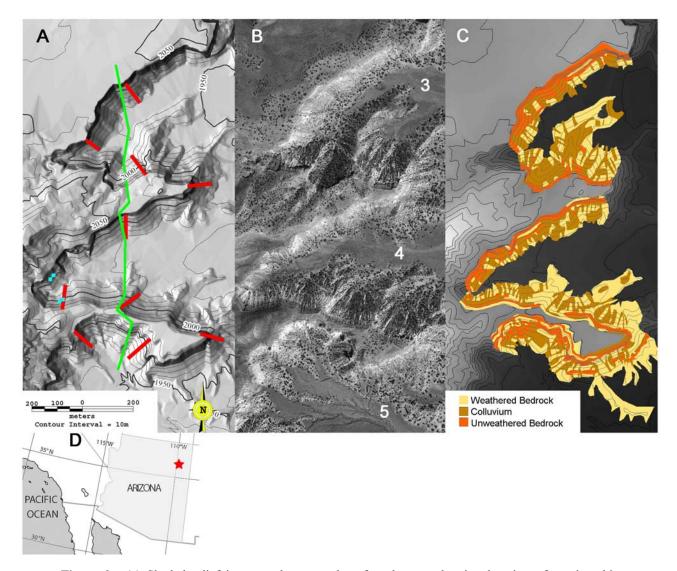
Figure 2. (a) Shaded relief image and topography of study area showing location of stratigraphic sections (red bars), sensor locations (light blue points), and topographic profile (green line) in Figure 1b. (b) The 1997 NAPP air photo of the study area with basins numbered. (c) Map showing distributions of colluvium, weathered bedrock, and unweathered bedrock on the sideslopes. (d) Location map showing the southwestern United States. Study area is marked with a star.

Mesa are formed on the capping Toreva formation sandstones of the Cretaceous Mesa Verde group and the underlying Mancos Shale [*Franczyk*, 1988].

[6] The Salt Wash member of the Morrison formation underlies the majority of the sideslopes and consists of lenticular bodies of fluvial sandstone and lesser shale up to 10 m thick [*Anderson and Lucas*, 1994, 1997]. In basins 1–3, *Tillery* [2003] found that except for local resistant calcite-cemented concretions, the Morrison formation sandstones are cemented almost exclusively by smectite and kaolinite clays. Expansion and contraction of smectite cement and matrix during wetting and drying cycles causes granular disintegration [*Tillery*, 2003]. Where weathering exceeds erosion, a weathered mantle up to 20 cm thick develops over more competent sandstone (Figure 3). The weathered mantle has high infiltration rates [*Burnett*, 2004] and should rarely produce surface runoff. Unweathered bedrock slopes have very low infiltration rates and show clear evidence of

surface runoff generation, including rilling and stripping of the mantle on weathered slopes below.

[7] Steep Morrison formation slopes commonly have high drainage density. Gullies are typically shallow, but are somewhat more incised and integrated on north-facing slopes (Figure 2). Exposures of smooth unweathered sandstone (i.e., "slickrock") are common on upper slopes below cliffs. Debris-covered slopes are often mantled by pebble- to small-boulder-sized clasts of Dakota sandstone in a loamy matrix. Locally below cliffs, large Jurassic and Cretaceous sandstone blocks form bouldery talus. Slope debris derived solely from the Morrison formation is mostly of loamy texture, but ranges from silty clay loam to loamy sand. Where present, colluvium thickness averages ~60 cm, and tends to thin in the upslope direction. Active slope erosional processes observed in the study area include rockfall from cliffs (including slab failures and topples), small mass failures of colluvium, and surface runoff producing sheet-
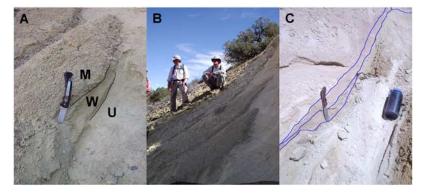
Figure 3. (a) Slope on sandstone with abrupt transition from a weathered mantle (W) to an unweathered (U) state in a small gully. A mobile layer (M) of weathered material transported from upslope is common on weathered surfaces. (b) Larger view of the slope in Figure 3a showing steep, bare sandstone slope above, where the weathered mantle has been stripped. (c) The lower line represents the modern slope-cliff contact, former positions of the contact are traced onto the cliff above. The conversion is occurring along a cliff parallel fracture. Other cliff parallel fractures, aligned roughly with fracture set 1 are exposed in the slope to the right.

wash, gullying, and locally small debris flows. Although sapping is often considered to be a major control on mass wasting of cliffs on the Colorado Plateau [*Howard et al.*, 1988], clear evidence of this process is rare within the study area. Most of the cliffs have very limited potential contributing area for groundwater discharge. Some salt precipitation occurs near the Cretaceous-Jurassic unconformity, but not at most lithologic contacts or slope-to-cliff transitions. The lower parts of high cliffs are often overhanging, which is commonly attributed to sapping, but in most cases there is no lithologic contact at the base of these cliffs that would localize discharge (Figure 4).

[8] Vegetation in the study area appears denser on north-facing slopes (Figure 1), as supported by visual estimates of percent cover [*Burnett*, 2004]. Trees are mostly piñon (*Pinus edulis*) and juniper (*Juniperus osteosperma*). Prominent grasses are blue grama (*Bouteloua gracilis*) and ricegrass (*Oryzopsis hymenoides*), and common shrubs include Utah serviceberry (*Amelanchier utahensis*), white sagebrush (*Artemisia ludoviciana*), and Stansbury cliffrose (*Purshia stansburiana*).

3. Methods

3.1. Bedrock Stratigraphy and Structure

[9] To examine whether changes in bedrock stratigraphy and structure might be responsible for differences in slope angles, ten stratigraphic sections were described through the Morrison and Dakota formations, including lithology, bed forms, and concretions (Figure 2a).

3.2. Insolation Modeling and Temperature and Soil Moisture Monitoring

[10] Given the hypothesis that differences in slope angles and valley asymmetry are a function of aspect-related differences in microclimate, we examined potential insolation differences on study area slopes using a model that incorporates daily changes in sun angle, incidence angle on topography, and topographic shading calculated from a 3-m DEM. Solar Analyst 1.0 (http://www.fs.fed.us/informs/, Helios Environmental Modeling Institute) was used to

model monthly and daily insolation for the year 2003. The model does not incorporate actual atmospheric conditions such as clouds and humidity that affect energy received at the ground, but parameters can be adjusted to
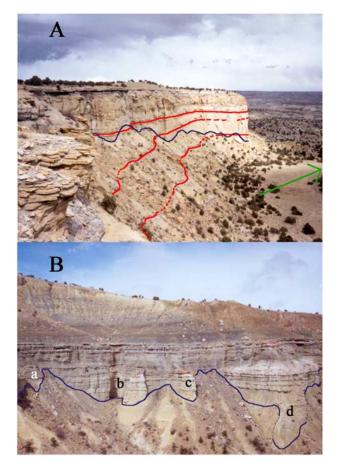

Figure 4. South-facing slopes of basins 3 and 4. (a) A dark line marks the slope-cliff transition and is crossed by lines marking shale units in basin 3. Arrow points downvalley. (b) This transition is lower in major gullies (marked by a and b) and bedrock ridges (marked by c and d).
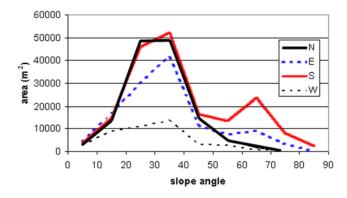
Figure 5. Slope angle distributions of canyon sideslopes calculated using the DEM.

model approximate average conditions. A diffuse proportion of 0.25 and transmissivity of 0.6 were used to represent mostly clear skies [*Fu and Rich*, 2000].

[11] We also measured air, surface, and shallow subsurface temperatures over a 1-year period using sensor arrays at four contrasting topoclimatic sites (Figure 2a). As water content is a fundamental control on weathering rates and plant growth, we installed soil moisture potential sensors at each array. Sensor arrays were installed at 1990–2000 m elevation on slopes of NW, NE, SE, and SW aspect in basin 4. The westerly arrays are on weathered bedrock slopes, whereas the easterly arrays are on colluvium-mantled slopes. Sensor arrays on the easterly colluvial slopes consist of (1) a shielded air temperature sensor 10 cm above the surface, (2) a surface temperature sensor, (3) a soil moisture sensor at 10 cm depth, and (4) a soil moisture sensor at 30 cm depth. The westerly arrays have the same air and surface temperature sensors, but only a shallow moisture sensor at 10 cm depth. The fourth sensor measured temperature at 10 cm depth within the weathered bedrock mantle.

[12] The sensors were installed in July 2002 and soil moisture sensors were fully equilibrated with the environment by 15 August. Data were collected at half-hour intervals for 1 year beginning 1 September 2002. Sensors recording with the same variable on opposite sides of the canyon were paired, and monthly and annual differences in temperature or soil moisture were calculated for each sensor pair by subtracting the north-facing slope record from the south-facing slope record. Average monthly temperatures were compared with those at Canyon DeChelly National Monument (1720 m elevation, 35 km east of Blue Gap) during the year of record and for 1974–2003 (Western Regional Climate Center, www.wrcc.dri.edu).

3.3. Slope Properties

[13] Field data collected to characterize slope properties at observation points include (1) location via global positioning system (GPS), (2) slope angle and aspect, (3) underlying bedrock formation and rock type, (4) surficial rock strength as a proxy for weathering and erodibility (primarily by surface runoff), (5) thickness of any weathered mantle and overlying debris, and (6) plant types and estimated percent vegetation cover. Slope angle and aspect were measured by Brunton compass for over 400 slope facets. Facets were defined as an approximately planar area of

slope with consistent angle and aspect, therefore vary in surface area depending on slope complexity. The field-collected slope facet data are more accurate for small areas than the DEM-derived data described below, and are thus useful in comparison of more complicated slopes, but exclude cliffs because of difficult access. For each facet, slope type was classified as unweathered bedrock, weathered bedrock or colluvium. Colluvial debris cover thickness was measured, or estimated if thicker than 30 cm. Where the debris cover was thin, patchy, or absent, the bedrock surface was classified as unweathered if a Schmidt hammer rebound value was registered at the surface (corresponding to a Young's modulus of >0.16 MPa), or weathered where a Schmidt hammer reading could be taken only at a depth of 1 cm or more.

[14] Slope orientation data were also derived from a 3-m resolution digital elevation model (DEM) produced using photogrammetry on three National Aerial Photography Program (NAPP) air photos (Figure 2). For analysis, the DEM was clipped to include only the canyon sideslopes. Average slope angles derived from DEMs decrease at coarser resolutions because of smoothing of slopes [*Gao*, 1997], therefore the 3-m DEM was used to improve resolution over 10-m USGS DEMs. ArcGIS 8.x was used to calculate the steepest slope, aspect, and surface area of each cell. The three slope types (unweathered bedrock, weathered bedrock, colluvium) were field-mapped at 1:6000 scale and imported to ArcGIS 8.x for DEM analysis. The field map is not fully accurate to 3 m, but 9-m features show up clearly, and this resolution was used only for calculations involving slope-type categories.

[15] Angle and aspect data were used together to test for significant differences in slope angle as a function of aspect. The distribution of the slope data is bimodal, with modes of 30–40° and 60–70° (Figure 5). Data must be normally distributed to use parametric T tests to compare the means of different slope angle distributions, thus we used the Shapiro-Wilk test to determine normality of the slope angle distributions.

3.4. Bedrock Surface Strength and Physical Properties

[16] To provide proxy data for the degree of weathering and erodibility of bedrock surfaces, we used standard engineering techniques for estimating rock strength. A type N Proceq Schmidt hammer was used to measure rock strength (elasticity) for 200 of the field-defined slope facets [e.g., *Hucka*, 1965; *Selby*, 1980; *Sjöberg and Broadbent*, 1991]. For each facet, up to 15 Schmidt hammer rebound measurements were taken within a ~3 m diameter and averaged, and a corresponding Young's modulus was estimated using a relationship for sandstones and limestones [*Katz et al.*, 2000]:

$$\ln(E) = -8.967 + 3.091 \times \ln(R) \left(r^2 = 0.994\right) \qquad (1)$$

where E is Young's modulus and R is Schmidt hammer rebound value.

[17] If bedrock was at or within 30 cm of the surface, the lithology was noted and rock strength measured. Weathered bedrock that was too soft for a measurement was excavated until either a measurement could be taken ($R > 10$ or $E > 0.16$ GPa) or a maximum depth of 30 cm was reached. The
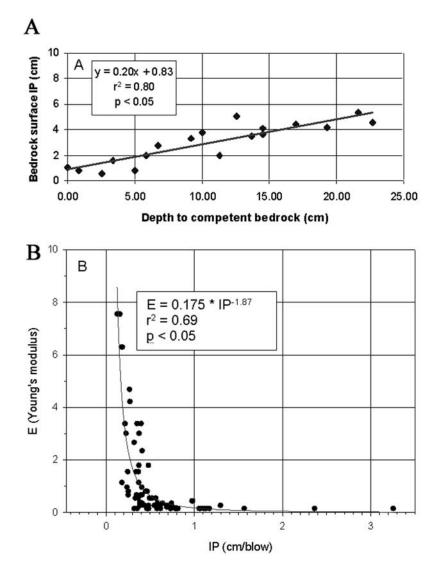
Figure 6. (a) Linear correlation between the weakness of the uppermost weathered bedrock (dynamic cone penetrometer incremental penetration (IP)) and the depth at which the Schmidt hammer yielded a measurable result. (b) Power law correlation between IP and Young's modulus derived from Schmidt hammer measurements taken after the penetrometer profile was excavated.

depth to competent bedrock ($R > 10$ or $E > 0.16$ GPa) was measured on these slope facets. To scale the strength of weathered bedrock to Young's modulus, over 30 dynamic cone penetrometer (DCP) profiles [*Webster et al.*, 1992] were obtained. The penetrometer was excavated after each test and Schmidt hammer readings taken throughout the profile. A strong linear correlation was observed between depth to competent bedrock (i.e., the first detectable Schmidt hammer reading) and incremental penetration (IP) measured with the DCP ($r^2 = 0.80$, $p < 0.05$). This was used to assign IP values to facets where rock strength could only be measured below the surface.

[18] Schmidt hammer values from the DCP profiles were then used to develop a correlation between rock strength (Young's modulus) and IP at the same depth (Figure 6). The Young's modulus data span several orders of magnitude, and power law functions typically provided the best fit of any models tested, though not all assumptions were met for the regression. The IP values assigned to facets with

weathered bedrock at the surface were thus converted to Young's modulus.

[19] Nine Morrison sandstone hand samples of variable strength (0.018–16 MPa) were collected to examine relationships between rock strength, bulk density, and physical properties relating to weathering. Bulk density was measured by two methods. Seven samples were cut into rectangular prisms and their volume and mass measured. All samples were also coated with paraffin wax, and their masses in air and water were measured. The samples were then made into thin sections. Point count methods developed specifically for sandstones [*Cochran et al.*, 1986] were used to determine the proportion of quartz, feldspar, lithics, cement, pore space and clay-rich matrix. The samples were generally fine-grained, subrounded, subarkosic wackes [*Burnett*, 2004]. Grain counts were used to determine rounding, grain size, and the average number of point and tangential contacts between grains [*Pettijohn et al.*, 1973]. A tangential contact exists where the edges of two grains are
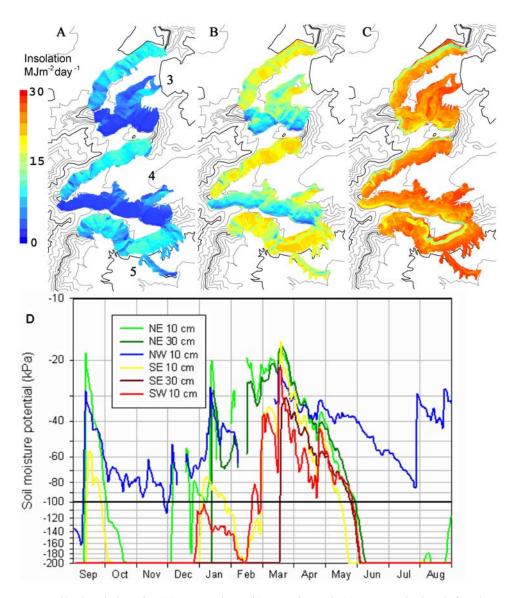
Figure 7. Daily insolation for (a) December, (b) March, and (c) June calculated for the canyon sideslopes using the Solar Analyst model. (d) Soil moisture recorded from September 2002 through August 2003. The NW and SW sensors were in bedrock, and the NE and SE sensors were in colluvium.

flush, whereas a point contact is where only a corner of a grain touches another grain.

4. Results

4.1. Bedrock Stratigraphy and Structure

[20] Bedrock is well exposed throughout the study area, allowing correlation between stratigraphic sections, although smaller lenses typically pinch out between sections. The units dip slightly (<5°) to the southwest (Figure 1b). No significant faults exist, but three main sets of nearly vertical joints or fractures were revealed by measurements in unweathered bedrock [*Burnett*, 2004]. Sandstones comprise 60–80% of each stratigraphic section, and sandstone proportion did not vary significantly between sections on north-facing slopes (75%) and south-facing slopes (73%). These observations indicate that valley asymmetry is highly unlikely to be related to differences in rock type across

valleys. Potential effects of bedrock stratigraphy and structure on valley asymmetry are further discussed below.

4.2. Topoclimatic Differences With Aspect
4.2.1. Insolation Modeling

[21] Output from the Solar Analyst model exhibits strong contrasts in insolation related to aspect and seasonal changes, both over the entire DEM and for the specific sensor locations (Figures 7 and 8). In June, overall insolation reaches a maximum, and north- and south-facing slopes receive similar radiation. Contrasts grow rapidly over the summer, however, and the largest differences in insolation between aspects occur in fall and winter months.
4.2.2. Temperature and Soil Moisture

[22] Temperature and soil moisture data from the NW, NE, SE, and SW-facing arrays show significant differences that are consistent with insolation contrasts among these aspects. Annual mean temperature differences between
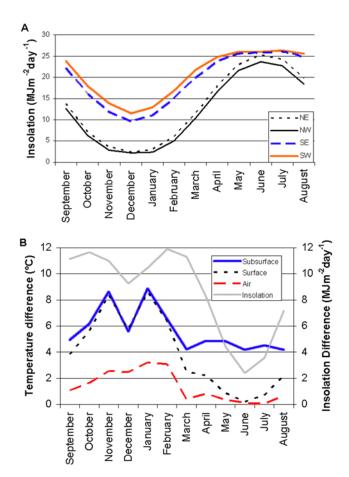
Figure 8. (a) Daily insolation for each month calculated for the facets that the four sensor arrays are installed on (labeled by aspect). (b) Average daily temperature and insolation differences between the two sensor networks on weathered bedrock for each month (southwest-facing sensor minus northwest-facing sensor).

paired sensors ranged from 1.4 to 5.6°C warmer at the sensors with southerly aspects (Table 1). Differences were greatest at the subsurface temperature sensors and least in the air sensors. Temperatures differences between north- and south-facing sensors are maximized with low sun angles in winter months, when daily mean temperatures were as much as 8°C higher at the south-facing surface and subsurface sensors (Figure 8b). Temperature differences are lower during the late spring and summer months, but south-facing aspects were still warmer over most of this period, and the subsurface sensors consistently remained about 4°C warmer. Temperature differences at the sensor locations mimic differences in daily insolation at those locations (Figure 8b). The insolation model correlates best with surface temperature differences between sensors on north- and south-facing slopes (Pearson $r^2 = 0.78$, $\alpha < 0.05$).

[23] Average temperatures recorded in the field for the year were 0.2°C cooler than at Canyon DeChelly National Monument but closely mimic temperature changes there [*Burnett*, 2004]. Temperatures were 1.1°C warmer than the 30-year average at Canyon DeChelly, and 2003 was the warmest on record at the time, with the most anomalous months being January, May, and July. At both Canyon

DeChelly and the field site, these months were all more than 3.0°C warmer than the 30-year average.

[24] Freeze-thaw cycles were calculated from each temperature record using two algorithms. First, each day when the temperature dropped below freezing was counted. Air and surface temperatures experienced many such freeze-thaw cycles during the winter. Southwest aspects experienced the fewest cycles, otherwise differences between aspects are not obvious. Subsurface sensors at 10 cm depth in bedrock recorded 0°C temperatures in only a few cycles, on westerly aspects [*Burnett*, 2004]. Second, each time the temperature dropped below −5.0°C and returned to above 0.0°C was counted as a single cycle, as frost wedging is most effective at −5.0 to −14.0°C [*Walder and Hallet*, 1985]. About 9–27% of the air and surface cycles reached a minimum temperature of −5.0°C, but neither subsurface temperature sensor recorded a value that low [*Burnett*, 2004].

[25] The soil moisture data are not likely to represent long-term average conditions, as precipitation for the year of record was 164 mm at Canyon DeChelly, only 46% of the mean of 240 ± 84 mm. Nonetheless, seasonal soil moisture changes and contrasts among aspects are quite instructive. Soil moisture remained relatively high from January through April (Figure 7d). Only the northwest-facing sensor, however, retained moisture from the winter through most of the summer. Large summer and fall rain events (e.g., 29 July and 9 September) also had a profound effect on moisture over subsequent weeks. Soil moisture differences between north and south aspects are greatest during the early summer and fall, before and after the summer monsoonal period, and when temperatures are high. Although insolation differences between the SW and NW sensor sites are largest in winter, soil moisture differences were less pronounced, most likely because low temperatures minimize evaporation and transpiration. Gaps in the north-facing records exist when the ground froze.

[26] Many weathering processes are controlled by changes in water content, which are greatest above −100 kPa [*Brady and Weil*, 2000]. The northwest-facing bedrock sensor experienced 14 wetting cycles of at least 10 kPa in magnitude above −100 kPa, whereas the other sensors experienced 8 or fewer of these cycles. This soil moisture sensor also recorded more than twice as many days above −100 kPa as any other sensor, and the south-facing sensors recorded the fewest. Overall, the soil moisture data indicate large differences in moisture availability for near-surface weathering that are consistent with aspect-related differences in insolation and temperature.

4.3. Slope Properties
4.3.1. DEM Slope Angles
[27] The DEM covered 482,148 m^2 and included 42,587 cells, with mean cell area 11.3 m^2. Cells were classified in four groups corresponding to each cardinal direction, e.g.,

Table 1. Annual Mean Temperature Differences[a]

	Subsurface	Surface	Air
SE−NE	...	3.2	2.1
SW−NW	5.6	3.9	1.4

[a]Given in °C.

Table 2. T Tests for Differences in Mean Slope Angles in the DEM[a]

	Mean (°) [n]	West-Facing	South-Facing	East-Facing
Mean (°) [n]		26.6 [4009]	30.7 [13493]	29.2 [10361]
North-facing	29.4 [12689]	**<0.01**	**<0.01**	0.14
East-facing	29.2 [10361]	**<0.01**	**<0.01**	
South-facing	30.7 [13493]	**<0.01**		

[a]The two-tailed p value for each test is shown. Significant results are bold.

Table 4. Mann-Whitney U Tests for Differences in Median Slope Facet Angles[a]

	Median	West-Facing	South-Facing	East-Facing
Median		41°	39°	36°
North-facing	37°	**<0.01**	**0.02**	0.15
East-facing	36°	**<0.01**	**<0.01**	
South-facing	39°	0.23		

[a]The two-tailed p value for each test is shown. Significant results are bold.

east-facing aspects have azimuths between 46 and 135°. In places where cliffs are observed in the field, the DEM typically showed slopes in the 60–90° range. For this analysis, we defined cliffs as slopes of > 60° [*Small and Clark*, 1982]. In order to enable comparisons between the DEM and facet data, and to normalize distributions, we first excluded cliffs from the statistical analysis of slope angles. The distribution of cliffs with aspect is also of obvious importance, and is discussed later.

[28] The DEM data populations are very large, and although not strictly normal, Shapiro-Wilk coefficients are very high (>0.98), so parametric T tests were used to assess differences in mean slope angle between aspects (Table 2). The differing area of individual cells due to slope angle is not accounted for, but this effect is minimal when skewness is low and high slope angles are removed. The mean angle of south-facing slopes is slightly (≤1.4°) greater than on other aspects, and T tests indicated small but significant differences between aspects except between north-and east-facing slopes, which only differed by 0.2°.

4.3.2. Facet Slope Angles

[29] Slope angle distributions of slope facets measured in the field are not normal for any of the four aspect classes. Removing outliers (defined as $>2\sigma$ from the mean, outside of the 2.5–97.5 percentile range, or more than 8° from the remaining data) reduced standard deviation, kurtosis, and skewness values, so that Shapiro-Wilk coefficients indicated that all but the west-facing data could be used in parametric tests. Most outliers were high values from near the slope-cliff transition, likely influenced by cliff-forming processes. Means of north- and east-facing slope facet angles are not significantly different from each other, but both are significantly steeper than the south-facing slopes (Table 3). As with mean slope facet angles, nonparametric Mann-Whitney U test showed that median angles of north- and east-facing facets are similar (Table 4). South- and west-facing facets are also not significantly different from each other, but both are significantly steeper than the north- and east-facing facets.

4.3.3. Comparison of DEM and Facet Slope Angles

[30] Differences in the nature of the DEM and slope facet data must be considered in interpretation. The DEM covers all valley sideslopes, and slope values are measured for a large number of cells with known surface areas. By com-

Table 3. T Tests for Differences in Mean Slope Facet Angles[a]

	Mean	South-Facing	East-Facing
Mean		40.3°	35.6°
North-facing	37.1°	**0.01**	0.18
East-facing	35.6°	**<0.01**	

[a]The two-tailed p value for each test is shown. Significant results are bold.

parison, field definition of facets is somewhat subjective, and data populations are 2 orders of magnitude smaller. Nonetheless, direct field measurements of slope angle and aspect are more accurate than DEM data, and include small-scale features that are smoothed in the DEM. Statistics on slope facets are biased toward smaller, typically steeper slope areas, since these are more common than large, smooth slope areas.

[31] Mean and median slope angles for the DEM were lower than those for slope facets (Tables 2, 3, and 4). This can be attributed to both smoothing in the DEM and the bias in facet data toward short, steep slopes. South- and west-facing slopes show larger disparities between angles from the two methods, so it is likely that these slopes have more short, steep facets. Slope facet data also exhibit a greater difference in angles between north- and south-facing slopes (about 3°), as compared to the DEM (1.3°) because these smaller-scale features are emphasized. West-facing slopes have the greatest difference in slope angle between the two methods. They are the steepest set of facets, but have the lowest angle by area in the DEM, where west-facing slopes are dominated by two large areas of relatively gentle slope. In contrast, most west-facing facets are small, steep gully walls. In the DEM, only 54 of 113 gullies identified in the field could be discerned, again illustrating the greater accuracy of field observations.
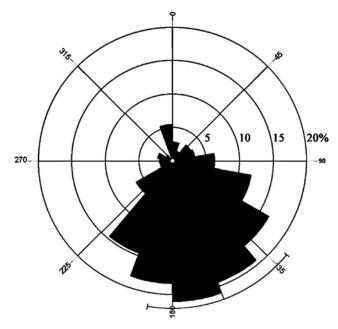

Figure 9. Rose diagram of cliff proportion (vertical cliff area divided by vertical slope area) with the mean vector (161°) and radial variance (32°).

Table 5. Slope Surface Area and Calculated Vertical Area Covered by Slopes and Cliffs

	Area (m^2)			Vertical Area Component (m^2)		
	Slope	Cliff	Percent Cliff	Slope	Cliff	Percent Cliff
All slopes	433176	48972	10	217771	45162	17
North-facing	134402	1914	1.4	67007	1735	2.5
East-facing	110687	11960	10	55229	10961	17
South-facing	146294	34216	19	76350	31663	29
West-facing	41793	882	2.1	19185	802	4.0

4.3.4. Cliff Area and Aspect

[32] The proportion of cliffs in the DEM varies dramatically by aspect (Figure 9; Table 5). South-facing slopes have nearly twice the mean cliff area for all aspects, whereas north-facing slopes have a very small proportion. East-facing slopes have a cliff proportion similar to the average for all aspects. Because the canyons drain east, west-facing cliffs are uncommon. Cliff proportion calculated using only the vertical component of DEM cell area also shows a much greater cliff area on south faces (Table 5). All proportions are significantly different using a Z test for proportions.

4.3.5. Slope Type

[33] Slope type (unweathered bedrock, weathered bedrock, and colluvium) varies dramatically between different aspect groups and measurement methods (Figure 10). South-facing slopes have the least weathered bedrock and the most unweathered bedrock, whereas north-facing slopes have the least unweathered bedrock. The DEM and facet data agree for north- and east-facing slopes, but a large disparity exists between the two methods for south- and west-facing slopes. South- and west-facing facets have a larger proportion of unweathered bedrock, and less weathered bedrock and colluvium, than calculated for the same aspects in the DEM. These differences are again consistent with the observation that many west-facing facets are short, steep gully walls of unweathered bedrock not represented in the DEM data.

[34] The three slope types also have distinct slope angle distributions calculated using the DEM. Weathered bedrock and colluvial slopes show similar slope angle distributions, except that weathered bedrock dominates the least steep slopes and has a mode slightly less than that for colluvial slopes (Figure 10c). Unweathered bedrock has a bimodal distribution, where the higher mode represents steep, bare bedrock slopes and cliffs. The lower mode is near the angle of repose, suggesting a former debris cover, but unweathered bedrock makes up very little of the gentler slopes (Figure 10c).

[35] The distribution of colluvium on major gully walls also varies by aspect (Figure 10d). Of 113 total, gully wall facets with easterly aspects are more commonly mantled by colluvium ($n = 68$) than are west-facing facets ($n = 16$); 29 gullies had an even distribution of colluvium. All proportions were significantly different at $\alpha = 0.05$ using a Z test for proportions.

4.4. Bedrock Surface Strength and Physical Properties

[36] Low Shapiro-Wilk coefficients indicate that rock strength distributions are not normal (Figure 11). Extreme
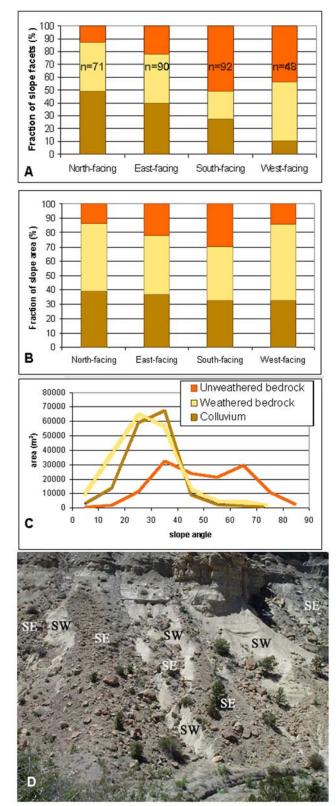

Figure 10. (a) Slope-type distribution for slope facet data. (b) Slope-type distributions calculated in the DEM. (c) Slope angle distributions for the three slope types calculated using the DEM. (d) South-facing slope of basin 4 near the head of the canyon. Note that colluvium is more common on southeast-facing slopes (SE) and bedrock is exposed over more of the southwest-facing slopes (SW).
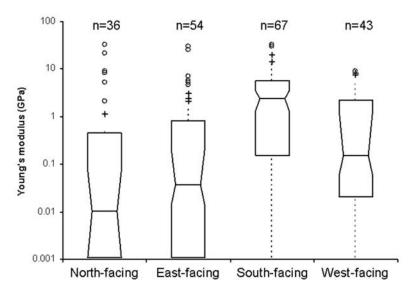
Figure 11. Distributions of bedrock strength data collected with a Schmidt hammer and grouped by aspect. Medians are marked by a horizontal bar within the boxes. Boxes extend from the lower quartile to the upper quartile. The interquartile range (IQR) is the range between the upper and lower quartile. Whiskers extend through data within 1.5 IQRs of the median, and circles represent high strength measurements that are more than 3 IQRs above the median.

high values are numerous (Figure 11) and typically represent unweathered bedrock on steep facets transitional to cliffs. The nonparametric Mann-Whitney U test shows that bedrock on north-facing slopes is similar to east-facing slopes, but is significantly weaker than on west- and south-facing slopes that have less moisture available for weathering. The difference between east- and west-facing slopes is not significant (Table 6).

[37] Sandstone samples show weathering-related changes that markedly reduce rock strength. The sandstones are largely cemented by clay (2–11%) and to a lesser extent by hematite (1–3%). Correlations between rock strength, density, pore space, cement, matrix and average number of grain contacts show that as the sandstones weather, they become weaker, less dense, and less grain supported (Figure 12). The relationship between rock strength and bulk density is well modeled by a power law equation with Spearman r of 0.97 (Figure 12). Correlations between rock strength and pore space are weaker but still significant. No significant relationships were found between rock strength and sand grain mineralogy or matrix content [*Burnett*, 2004], however, suggesting that chemical weathering is insignificant, at least in comparison with primary mineralogical variability. Morrison sandstone weathering appears to primarily cause volumetric expansion, resulting in reduced density and grain contacts and an increase in pore space.

5. Discussion

[38] Greater weathering and lower rock strength on northerly aspects is consistent with a strong control of bedrock erosional resistance through hydration weathering, since northerly aspects have lower insolation and more soil moisture retention. Accordingly, the proportion of cliff area is much higher and noncliff slopes are slightly steeper on southerly aspects, where weathering is reduced and rock strength is greater. Topoclimatic differences and result-

ing slope characteristics are discussed below, and process-oriented models of slope evolution are discussed further below with emphasis on implications for long-term slope evolution.

5.1. Topoclimatic Contrasts With Aspect

[39] Annual air temperatures on south-facing canyon slopes in the study area were 1.4–2.1°C warmer than north-facing slopes (Table 1), and differences in winter were 2–3°C warmer (Figure 8). Modern vertical temperature gradients in the southern Colorado Plateau are 5–6°C/ 1000 m [*Stute et al.*, 1995], thus air temperature differences among aspects (Table 1) are roughly analogous to elevation differences of about 230–600 m. Paleoclimatic reconstructions for the southern Colorado Plateau and adjacent areas indicate a 2–4°C range of mean annual temperatures in the Holocene, and late Pleistocene temperatures 4–6°C cooler than present [*Phillips et al.*, 1986; *Cole*, 1990; *Davis and Shafer*, 1992; *Anderson*, 1993; *Stute et al.*, 1995; *Zhu et al.*, 1998]. Temperature differences between north- and south-facing slopes thus approach long-term differences in Holocene mean temperatures, but both analogies are limited. For example, precipitation generally increases with elevation, and late Quaternary climate changes are likely associated with precipitation changes as well. In contrast, topoclimates on opposing aspects have small precipitation differences, and temperature contrasts change dramatically over the

Table 6. Mann-Whitney U Tests for Differences in Median Young's Modulus[a]

	Median (GPa)	West-Facing	South-Facing	East-Facing
Median (GPa)		0.16	2.36	0.04
North-facing	0.01	**0.01**	**<0.01**	0.14
East-facing	0.04	0.10	**<0.01**	
South-facing	2.36	**<0.01**		

[a]The two-tailed *p* value for each test is shown. Significant results are bold.
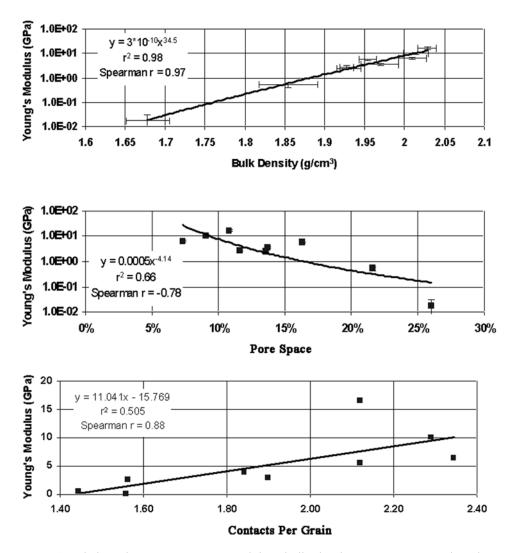
Figure 12. Correlations between Young's modulus, bulk density, pore space, and grain contacts measured in nine Morrison formation sandstones.

seasons. Numerical modeling of desert soils, however, implies that a temperature decrease of 4°C, with no precipitation increase, significantly increases infiltration depth, leaching, and weathering rates [*McFadden and Tinsley*, 1985].

[40] Ultimately, soil moisture is likely the most important aspect-influenced control on weathering and slope form in the study area. Differences in field-measured moisture potential are probably most related to differential evapotranspiration driven by insolation and temperature [*Kirkby et al.*, 1990], as both latent heat transfer and evaporation are proportional to temperature and net radiation [*Barry and Chorley*, 1998]. Lower soil moisture is observed on south aspects during the warm season except during brief periods in the summer monsoon (Figure 7d). Evapotranspiration is higher on south-facing slopes, as indicated by more rapid drying after storm events and during the spring. In contrast, only the north-facing sensor on bedrock indicated a relatively high potential all year. Soil moisture potential is highest in winter, but the contrasts between aspects are smallest, even though insolation and temperature differences between north- and south-facing slopes reach their

highest magnitude with low-angle winter sun. With lower temperatures, winter evapotranspiration is generally lower than precipitation, and soil moisture increases on all slopes, reducing differences between north and south aspects.

[41] Windward slopes experience greater precipitation and evapotranspiration [*Barry and Chorley*, 1998], but the net effect of wind on soil moisture in the study area is unknown. Prevailing winds indicated by Holocene eolian features in northeast Arizona [*Stokes and Breed*, 1993] and northwest New Mexico [*Wells et al.*, 1990] are southwesterly. Wind direction during storms is much more variable. It is not likely that wind-generated precipitation contrasts between north and south slopes are large, as the study area canyons probably channel winds subparallel to both aspects.

[42] Only a relative assessment of the effects of soil moisture on slope vegetation can be made, as the permanent wilting point for plants is about −1500 kPa [*Brady and Weil*, 2000], well below the minimum potential resolved by the field instruments (−200 kPa). Calculations of evapotranspiration, potential evapotranspiration and water stress are also impossible without humidity data. Higher potential at north-facing sensors implies less water stress, particularly

during the summer, which likely allows for almost three times greater vegetation cover on north aspects than on south-facing slopes [*Burnett*, 2004].

5.2. Slope Processes and Asymmetry

[43] Excluding cliffs, the mean angle of south-facing slopes is statistically greater than north-facing slopes, but differences are quite small. Slope gradients range broadly around the angle of repose (Figure 5) and are controlled over substantial areas by the mobility of the cover of weathered bedrock and colluvium. Many unweathered bedrock slopes lie near the angle of repose as well (Figure 10c) and were probably covered by a weathered mantle or colluvium in the recent past. Some unweathered bedrock slopes well exceed the angle of repose, however, and grade into cliffs, and gentle slopes exist on highly weathered sandstone and shale. If the small aspect differences in noncliff slope angles between north and south slopes are real, they probably relate to these weathering and bedrock strength contrasts. The difference in cliff area between north- and south-facing slopes, however, is very large (Table 5) and is the principal element of asymmetry within the canyons. Cliffs of 5–70 m height exist along the entire length of south facing-slopes except at one place in western basin 5. In contrast, north-facing slopes have no cliffs higher than 1–2 m, except in narrow canyon heads.

[44] Asymmetry in the study area canyons has similar aspect relations to that in the South Dakota badlands on weak rocks [*Churchill*, 1982], and is most likely the result of topoclimatically controlled weathering and erosion processes. Enhanced weathering and debris formation on north-facing slopes keeps slope angles lower by providing more erodible surface material, rapidly reducing ledges, and minimizing the area of cohesive bedrock that can hold steep slopes. Bedrock on little-weathered south-facing slopes, however, is strong enough to hold cliffs at least 70 m high, and noncliff slopes are also slightly steeper on average.

[45] In contrast, asymmetry documented elsewhere in the western U.S. is often characterized by steeper north-facing slopes [*Melton*, 1960; *Dohrenwend*, 1978; *Branson and Shown*, 1989; *McMahon*, 1998]. This pattern has been attributed largely to greater vegetation density on moister north slopes that (1) reduces runoff through increased rainfall interception, infiltration rates, and surface roughness and (2) increases erosion resistance through root strength [*Melton*, 1960; *Selby*, 1993; *Schmidt et al.*, 2001]. As in *Churchill*'s [1982] badlands study, however, vegetation cover in our study area is low even on north-facing slopes [*Burnett*, 2004], with limited effect on erosion by surface runoff. Nevertheless, the greater vegetation cover on north-facing slopes may somewhat moderate slope angle asymmetry.

[46] By itself, bedding within 10° of horizontal has limited effect on slope stability [*Selby*, 1980, 1993], but given sapping processes, even slight inclination of a caprock unit may produce slope asymmetry with a steeper scarp slope facing away from the dip direction [*Howard and Selby*, 1994]. The slight southwesterly dip of the strata in our study area, however, would tend to favor cliffs on north-facing slopes, opposite of the pattern we document. In addition, asymmetry with steeper south faces exists where only the Morrison formation is present, and is also quite

apparent in basins 1 and 2 where the Dakota caprock is completely absent. Caprock cliffs in the study area may be either Dakota or Morrison formation sandstones. Erosion of the weaker rocks below undermines cliffs [*Howard and Selby*, 1994], and cliff height in our study area is probably largely a function of weathering and erosion rates on the underlying slopes.

[47] An aspect of asymmetry that is apparent but unquantified is the greater development of stream drainages on north-facing slopes (Figure 2). This may result from the greater area for surface runoff generation on slopes as opposed to cliffs, as well as greater erodibility of more weathered north-facing slopes. Also, once a major cliff develops, focused headward erosion along a drainage is limited by the cliff face itself.

5.3. Morrison Formation Weathering

[48] Because slope processes in the study area change dramatically with weathering, we further consider weathering processes and effects. With progressive weathering of Morrison formation sandstones, Young's modulus and bulk density are reduced, and porosity increases. Strength reduction probably results from both loss of cohesion in the clay cements and reduced grain contact friction. Progressive reduction in bulk density requires mechanisms that expand the pore spaces (Figure 12) and (or) isovolumetrically remove mass without substantial compaction. There is no reduction in cement or matrix with weathering, but more weathered samples are less grain supported, indicating significant rock expansion [*Burnett*, 2004]. If mass is lost by leaching, it is likely small and subordinate to physical weathering by expansion. Frost action and the swelling of clays are two processes that can cause volumetric expansion.

[49] The specific processes involved in frost action are poorly understood for soft, porous rocks. Frost action in most bedrock requires temperatures of −5°C and −10°C and moisture conditions near saturation [*Walder and Hallet*, 1985; *Matsuoka*, 1990], but strain experiments [*Matsuoka*, 1988] in porous rocks indicated that most expansion occurs between 0 and −5°C. Winter surface temperatures in the study area often fell below freezing, and frost heave has been observed in the upper 1 cm of slope debris, but temperatures at 10 cm depth in weathered bedrock rarely cooled below 0°C and never reached −5°C, even with a 1–2°C correction for warmer than average temperatures in winter 2002–2003. The bedrock never reached saturation (>−10 kPa), but was relatively moist (>−100 kPa) on north faces all winter and on south faces March through May (Figure 7d). Soil moisture in colluvium also decreased with depth (Figure 7d), implying that frost action could not be responsible for producing >30 cm thick weathered mantles on bedrock. Temperature and moisture conditions are unfavorable for frost action below a few centimeters depth, but could accelerate breakdown of near-surface materials.

[50] In contrast, *Schumm and Chorley* [1966] inferred that frost action was the most important weathering process causing disintegration of sandstone talus on the Colorado Plateau. They measured mass loss of boulders exposed to natural weather augmented by simulated rainfall over ∼1.5 year in Denver, Colorado. The most mass loss per unit precipitation occurred with freeze-thaw cycles, but with
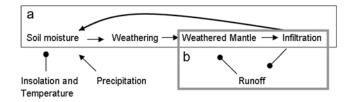
Figure 13. Feedbacks between the weathered mantle and the (a) soil moisture and (b) runoff systems. Arrow links indicate a positive relationship between the two elements joined, and a links that end in dots indicate a negative relationship between the elements.

reduced evaporation in winter, hydration would also be enhanced. Also, since precipitation was artificially doubled, the rocks were more likely near saturation during freeze-thaw cycles. The most rapid weathering occurred when 80 mm of simulated rainfall was applied during midwinter, and when the rocks were buried in intermittently melting snow. These are not common conditions in our study area, and in particular, saturated conditions are unlikely on moderate to steep bedrock slopes and cliffs. Frost action is probably most effective in talus weathering in our study area, consistent with *Schumm and Chorley*'s [1966] observations and experimental design.

[51] Swelling of smectite clays within the sandstones has been suggested as the primary weathering mechanism in the Morrison formation [*Tillery*, 2003] and in other clay-rich sandstones [*Vicente*, 1983]. X-ray diffraction analysis of Morrison sandstones reveals that the major clays are smectite and kaolinite [*Tillery*, 2003]. Swelling of smectites is directly related to the mass water content in soils [*Fu et al.*, 1990; *Cygan*, 2002]. Since volumetric and mass water contents in sandy materials change only slightly below −100 kPa [*Brady and Weil*, 2000], we assume that only fluctuations in moisture potential above this limit are important for smectite hydration. The period over which soil moisture potential is above −100 kPa or the number of wetting cycles recorded provide estimates of weathering potential, and both measures suggest that potential clay expansion on north-facing slopes is twice that of south-facing slopes [*Burnett*, 2004]. The moisture on north-facing slopes is also more likely to reach greater depths and produce thick weathered mantles.

[52] Clay expansion is also likely to be the dominant weathering process in shale units of the Morrison, Dakota, and Mancos formations. Weathered surfaces on these units exhibit "popcorn" morphology attributed to cycles of clay hydration [e.g., *Churchill*, 1982]. Shattered pieces of well-cemented Dakota sandstone comprise most of the coarse material in colluvium, showing that they weather much more slowly than Morrison formation sandstones.

5.4. Slope Processes and Implications for Landscape Evolution

[53] Repeat ground-based LiDAR measurements in the study area have shown that prolonged, intense precipitation causes significant erosion of the weathered sandstone mantle and some debris slopes [*Wawrzyniec et al.*, 2007]. The importance of heavy rainfall in stripping weathered material is supported by soil and dendrogeomorphic data in the study

area that indicate rapid erosion in major storms following prolonged droughts [*McAuliffe et al.*, 2006]. Once bedrock is exposed (e.g., Figure 3), surface runoff increases dramatically. These observations imply that two major positive feedbacks exist between weathering, erosion, infiltration and runoff on the Morrison formation (Figure 13). In feedback 1, increased soil moisture enhances production of a weathered mantle. This weathered bedrock increases soil moisture infiltration and retention that accelerates hydration weathering, and maintains or expands the mantle [cf. *Wahrhaftig*, 1965]. Feedback 1 is directly linked to evapotranspiration differences driven by topoclimatic contrasts in insolation and temperature and is largely responsible for the differences in weathering and rock strength observed on north- and south-facing slopes. Feedback 1 enhances weathering on moist north-facing slopes and increases erodibility, but reduces surface runoff, the primary agent of slope erosion.

[54] A second positive feedback (Figure 13) helps prevent development of a weathered mantle on unweathered bedrock. High runoff generation on unweathered slopes strips away weathered material below, maintaining or expanding the area of unweathered bedrock (Figure 3). Feedback 2 has the greatest effect where a drier topoclimate hinders weathering, and is negated where a thick weathered mantle limits runoff. The two feedbacks push slope evolution toward two end-member geomorphic expressions for this sandstone bedrock: (1) a transport-limited slope mantled by 10 to 30 cm of disintegrated bedrock and (2) an unweathered, sediment-limited bedrock slope. The observed behavior of this overall slope system is similar to that proposed by *Gilbert* [1877, p. 97], where presence of a soil mantle promotes water retention and further weathering (although weathering is thought to slow with increasing thickness); but where the mantle is stripped, weathering is negated. The system may thus be approximated by a "humped" curve of soil production rate as a function of soil depth, where the maximum production rate (by weathering) exists at some nonzero soil depth, and declines with either increasing or decreasing depth [*Carson and Kirkby*, 1972; *Ahnert*, 1976]. This system contrasts with models of exponentially declining soil production rate with soil depth proposed for more continuously soil-mantled landscapes, where the production rate is maximum at zero soil depth [e.g., *Heimsath et al.*, 1997].

[55] The prevalence of south-facing cliffs implies that steepening of drier bedrock slopes ultimately proceeds to a mass failure-dominated system. Slab failures and topples typically result from slope erosion removing support from cliff bases, where overburden stress is highest [*Selby*, 1982]. Runoff from cliffs may also promote slab failures by enhancing hydration weathering and erosion of the slopes near the base of a cliff, causing undercutting. Erosion processes therefore differ markedly with aspect. Neither feedback directly implies that long-term erosion rates are different with aspect, but if cliff retreat rate is controlled mainly by the rate of undermining by slope erosion below, then south-facing canyon walls may erode more slowly.

[56] The potential for gully incision and erosion is also enhanced by bedrock weathering, but buildup of coarse debris in channels inhibits flow and sediment transport, and armoring can lead to enhanced lateral erosion and channel
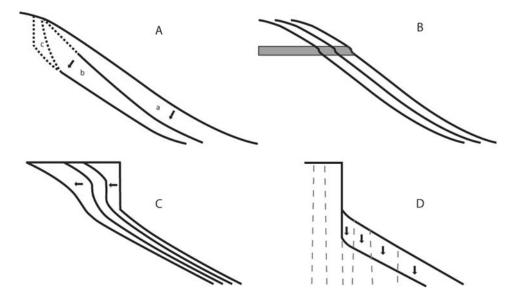
Figure 14. Cliff initiation from a slope. (a) Headward gully erosion produces a steep, unweathered upper slope (dotted lines a and b), which is ultimately undercut and fails along a nearly vertical fracture producing a cliff (line c). This process will continue and extend the existing cliff. (b) Where unweathered bedrock slopes are not extensive and not long-lived, slope parallel retreat occurs with only small ledges forming where resistant units (shaded area), typically Dakota Sandstones, outcrop. (c) Cliff reduction can occur where high weathering and sediment production rates on the cliff and upper slope reduce retreat rates of the lower slopes. (d) Cliff expansion is also aided where near-vertical unloading joints or tectonic fractures (dashed lines) facilitate slope weathering and provide a vertical erosional contact.

migration [*Bryan*, 1940; *Mills*, 1981; *Twidale and Campbell*, 1986]. East-facing gully sideslopes are gentler and more often debris covered than opposing west-facing sideslopes (Table 3, Figure 10). Material from the east sideslopes armors that channel wall, forcing undercutting of the less protected west-facing wall, resulting in a steeper sideslopes with more exposed bedrock, and eastward gully migration. This also undercuts any colluvial mantle on the adjacent east-facing slope, but the west-facing wall is too steep to maintain a debris cover, so that colluvium adds to the armor. Small debris flows are also common, and their deposits may have aided the armoring process in some gullies. These self-reinforcing processes produce short, steep bedrock slopes that are most common in the west-facing facet data.

[57] Cliff formation and destruction processes are clearly key in interpreting long-term landscape evolution in these canyons. Cliffs appear to begin as either steep unweathered Morrison slickrock slopes (Figure 3b) or as small resistant ledges in the Dakota formation. Where headward gully erosion or slopewash exceeds weathering on Morrison formation slopes, progressively stronger bedrock is exposed (Figure 14a, line a). Under low soil moisture, the upper slopes remain unweathered and become steeper, as they erode more slowly than the slopes below that receive runoff (Figure 14a, line b). The unweathered slopes expand laterally and vertically until failure occurs along tectonic or slope parallel unloading fractures (Figure 14a, line c). Where weathering exceeds erosion, steep slickrock slopes required for cliff initiation in the Morrison formation cannot form. Cliff initiation also occurs where Dakota or upper Morrison formation sandstones behave as erosion resistant caprocks. Slopes below the caprock continue to erode, leaving a cliff below the resistant unit until overburden stresses cause the weaker lower unit to fail [*Koons*, 1955]. Both of these processes are diminished on north-facing slopes that generally have enhanced moisture and weathering.

[58] Conversion of slopes to cliffs is rarely discussed in landscape evolution models, but is commonly apparent on south-facing slopes in these canyons. The slope-cliff transition is wavy and rarely follows lithologic contacts; continuous rock units pass laterally from cliff to slope and back to cliff (Figure 4). Depressions in the slope-cliff transition occur where erosion is enhanced by tributaries that drain over the canyon rim and by runoff from steep bedrock slopes (Figure 4). The contact is also depressed near the eastern mesa points, where two major cliffs intersect. The slope-cliff transition is thus controlled by weathering and erosion rather than by stratigraphy

[59] Once initiated, cliffs may expand downward by slope erosion combined with relative stability of the near-vertical face. Slab failure along stress fractures parallel to the cliff free face also facilitates rapid conversion of bedrock slopes to cliffs. Cliff parallel fractures were observed mostly in slopes below higher cliffs or those aligned with the main tectonic fracture set. The fractures also extend into bedrock below cliffs (Figures 3c and 14d) and aid infiltration, weathering and erosion of cliff-fronting slopes.

[60] On north-facing slopes, cliff reduction processes have clearly dominated. Enhanced weathering and debris accumulation on slopes below cliffs leads to a reduction in cliff height (Figure 14c), similar to classic slope decline and replacement models [*Davis*, 1899; *Penck*, 1924]. A persis-

tent weathered mantle or debris cover on moister north-facing slopes retards slope retreat and cliff expansion, instead promoting upward extension of the slope. The debris mantle shed from retreating Dakota sandstone caprock is unlikely to be the primary factor controlling long-term slope erosion, as present debris covers are thin mobile layers, and relict talus slopes or "flatirons" [*Howard and Selby*, 1994] are not present. Cliffs in the study area are not observed to buried by basal debris. Thus, valley asymmetry is largely a reflection of the net relative effectiveness of initiation, growth and reduction processes of cliffs, largely controlled by bedrock weathering and erosional processes on subjacent north- versus south-facing slopes. Modern topoclimatic contrasts are sufficient to place north- and south-facing slopes in different modes of development. Under modern and Holocene climates, cliff expansion has clearly been dominant on south-facing slopes, but north-facing slopes show more diversity, and some evidence for cliff initiation, growth and decline can be locally observed on slopes of all aspects at present.

[61] Although strongly suggestive, modern monitoring data cannot directly indicate whether topoclimatic differences were effective over timescales sufficient for slope evolution, under very different, pre-Holocene climates. Estimated slope retreat rates in the study area based on dendrogeomorphic analyses [*McAuliffe et al.*, 2006] and cosmogenic nuclide accumulation in Jurassic sandstone concretions [*McFadden et al.*, 2005] are similar at a few mm per year, despite $10-10^2$ and 10^3 year measurement timescales, respectively. Perhaps coincidentally, retreat rates over 10^7 year based on assumed post-Laramide initial escarpment positions are also a few mm per year [*Schmidt*, 1989]. These data suggest that major changes in slope morphology could occur over 10^4-10^5 years in the middle to late Quaternary.

[62] Although Pleistocene climates were not uniformly wetter than present, episodes of greater effective moisture may have favored cliff reduction and debris slope processes, with very little cliff area on north aspects. It is possible that at times in the Quaternary, cliffs were mostly erased from these canyons, with slopes covered by continuous debris blankets, as inferred on other Colorado Plateau escarpments [*Howard and Selby*, 1994], but no field evidence exists to test this. Modern debris slopes appear to be largely relict late Pleistocene features that are degrading, particularly on south-facing slopes where backwasting of the escarpment appears minimal at present. While some smaller south-facing cliffs may have formed entirely within the Holocene, many are too high for this to be the case given estimated rates of slope retreat and cliff formation. For example, cliffs in the eastern study area are up to 70 m tall, which requires an unlikely combination of vertical slope lowering of 7 mm a^{-1} (where a is years) and a virtually noneroding, downward-extending cliff, if restricted to the Holocene. Even faster slope lowering is necessary if some cliff retreat is allowed. Thus, some net growth likely occurred on those cliffs within the late Pleistocene.

6. Conclusions

[63] Topographically induced microclimate has had a profound effect on weathering, erosion and slope evolution

in canyons cut in the Morrison and Dakota formations in northeastern Arizona. Bedrock stratigraphy places an important but not overriding control on slope morphology. Aspect very strongly influences slope and cliff processes through differences in soil moisture, which plays a key role in weathering of Morrison formation sandstones. The predominantly smectite clay cement in these rocks [*Tillery*, 2003] undergoes hydration expansion weathering (Figure 12). Feedbacks between moisture, weathered mantle, and infiltration (Figure 13) enhance aspect-related differences in process and lead to major differences in erodibility of bedrock exposed opposing slopes (Figure 10). South-facing slopes receive more insolation (Figure 7) yielding generally warmer and drier conditions, and are only moist for a few months in the winter when evapotranspiration is lowest and after the snowmelt episodes in spring (Figure 7d). In contrast, the wetter north-facing bedrock slopes hold sufficient moisture to allow weathering throughout the year. Although greater plant cover on north aspects retards erosion and maintains steeper slopes in more densely vegetated areas of the western U.S. [*Melton*, 1960; *Branson and Shown*, 1989; *McMahon et al.*, 1996; *McMahon*, 1998], in our study area rock resistance has a greater influence, making less weathered noncliff slopes slightly steeper and promoting much greater cliff area on south aspects (Figure 9).

[64] Cliff initiation and expansion require exposures of unweathered bedrock at the surface and enhanced erosion caused by headward gully expansion, concentration of runoff from slickrock slopes, or run-on from slopes above the canyon. The high weathering rates on north-facing slopes inhibit cliff formation by preventing precursor unweathered slickrock slopes from forming. The small ledges and cliffs (<3 m) that are common on north-facing slopes, however, are potentially the result of warm, dry climates in the Holocene, given slope and scarp retreat rates of a few mm per year [*Schmidt*, 1989; *McFadden et al.*, 2005; *McAuliffe et al.*, 2006]. High cliffs (10–70 m) on south-facing slopes indicate that cliff expansion has been the dominant mode throughout at least the Holocene and latest Pleistocene. With wetter climatic episodes in the late Pleistocene, cliff formation would be lessened on most slopes, and cliff reduction or elimination would have likely occurred on north-facing slopes. Overall, aspect-related controls on slope evolution have played out in the context of long-term relief generation, escarpment retreat, and climatic change on the Colorado Plateau.

References

Ahnert, F. (1976), Brief description of a comprehensive three-dimensional process-response model of landform development, *Z. Geomorphol. Suppl.*, 25, 29–49.

Anderson, O. J., and S. J. Lucas (1994), Middle Jurassic stratigraphy, sedimentation and paleogeography in the southern Colorado plateau and southern High Plains, in *Mesozoic Systems of the Rocky Mountain*

Region, USA, edited by M. V. Caputo, J. A. Peterson, and K. J. Franczyk, pp. 299–314, Soc. Sediment. Geol., Denver, Colo.

Anderson, O. J., and S. J. Lucas (1997), The Upper Jurassic Morrison formation in the Four Corners region: Mesozoic geology and paleontology of the Four Corners region, paper presented at 48th Annual Field Conference, N. M. Geol. Soc., Albuquerque, N. M.

Anderson, R. S. (1993), A 35,000 year vegetation and climate history from Potato Lake, Mogollon Rim, Arizona, *Quat. Res.*, *40*, 351–359, doi:10.1006/qres.1993.1088.

Barry, R. G., and R. J. Chorley (1998), *Atmosphere, Weather and Climate*, 409 pp., Routledge, New York.

Brady, N. C., and R. R. Weil (2000), *Elements of the Nature and Properties of Soils*, 606 pp., Prentice-Hall, Upper Saddle River, N. J.

Branson, F. A., and L. M. Shown (1989), Contrasts of vegetation, soils microclimates, and geomorphic processes between north- and south-facing slopes on Green Mountain near Denver, Colorado, *U.S. Geol. Surv. Water Resour. Invest. Rep.*, *89-4094*.

Bryan, K. (1940), Gully gravure—A method of slope retreat, *J. Geomorphology*, *3*, 89–106.

Bull, W. B. (1991), *Geomorphic Responses to Climate Change*, 326 pp., Oxford Univ. Press, New York.

Burnett, B. N. (2004), Aspect and microclimatic influences on hillslope geomorphology, northeastern Arizona, M.S. thesis, 85 pp., Univ. of N. M., Albuquerque, N. M.

Carson, M. A., and M. J. Kirkby (1972), *Hillslope Form and Process*, 475 pp., Cambridge Univ. Press, Cambridge, U. K.

Churchill, R. R. (1981), Aspect-related differences in badlands slope morphology, *Ann. Assoc. Am. Geogr.*, *71*, 374–388.

Churchill, R. R. (1982), Aspect-induced differences in hillslope processes, *Earth Surf. Processes Landforms*, *7*, 171–182, doi:10.1002/esp.3290070209.

Cochran, A., J. M. Ajdukiewicz, M. J. Klosterman, F. C. Lin, S. T. Paxton, and J. O. Szabo (1986), *Standardized Point-Count Classification and Procedures for Sandstone Petrology*, Exxon Prod. Res.Co., Houston, Tex.

Cole, K. L. (1990), Reconstruction of past desert vegetation along the Colorado River using packrat middens, *Paleogeog. Paleoclim. Paleoecol.*, *76*, 349–366, doi:10.1016/0031-0182(90)90120-V.

Cygan, R. T. (2002), Interactions of biomolecules with clay minerals, in *Linking the Geosciences to Emerging Biological-Engineering Technologies*, edited by R. T. Cygan, C. K. Ho, and C. J. Weiss, *Rep. SAND2002-3690*, pp. 10–24, Sandia Natl. Lab., Albuquerque, N. M.

Davis, O. K., and D. S. Shafer (1992), A Holocene climatic record for the Sonoran Desert from pollen analysis of Montezuma Well, Arizona, USA, *Paleogeog. Paleoclim. Paleoecol.*, *92*, 107–119, doi:10.1016/0031-0182(92)90137-T.

Davis, W. M. (1899), The peneplain, *Am. Geol.*, *23*, 207–239.

Dohrenwend, J. C. (1978), Systematic valley asymmetry in the central California Coast Ranges, *Geol. Soc. Am. Bull.*, *89*, 891–900, doi:10.1130/0016-7606(1978)89<891:SVAITC>2.0.CO;2.

Franczyk, K. J. (1988), Stratigraphic revision and depositional environments of the Upper Cretaceous Toreva formation in the northern Black Mesa area, Navajo and Apache counties, Arizona, *U.S. Geol. Surv. Bull.*, *1685*, 1–32.

Fu, M. H., Z. Z. Zhang, and P. F. Low (1990), Changes in the properties of a montmorillonite-water system during the adsorption and desorption of water: Hysteresis, *Clays Clay Miner.*, *38*, 485–492, doi:10.1346/CCMN.1990.0380504.

Fu, P., and P. M. Rich (2000), *The Solar Analyst 1.0 User Manual*, 48 pp., Helios Environ. Model. Inst., Lawerence, Kans. (Available at http://www.fs.fed.us/informs/solaranalyst/solar_analyst_users_guide.pdf)

Gao, J. (1997), Resolution and accuracy of terrain representation by grid DEMs at a micro-scale, *Int. Geogr. Inf. Sci.*, *11*, 199–212, doi:10.1080/136588197242464.

Gilbert, G. K. (1877), *Report on the Geology of the Henry Mountains*, U.S. Geol. Surv., Washington, D. C.

Graf, W., R. Hereford, J. E. Laity, and R. A. Young (1987), The Colorado plateau, in *Geomorphic Systems of North America*, vol. 2, edited by W. Graf, pp. 259–302, Geol. Soc. of Am., Boulder, Colo.

Heimsath, A. M., W. E. Dietrich, K. Nishiizumi, and R. C. Finkel (1997), The soil production function and landscape equilibrium, *Nature*, *388*, 358–361, doi:10.1038/41056.

Howard, A. D., and M. J. Selby (1994), Rockslopes, in *Geomorphology of Desert Environments*, edited by A. D. Abrahams and A. J. Parsons, pp. 123–172, Chapman and Hall, London.

Howard, A. D., R. C. Kochel, and H. E. Holt (1988), *Sapping Features of the Colorado Plateau: A Comparative Planetary Geology Field Guide*, 108 pp., NASA, Washington, D. C.

Hucka, V. (1965), A rapid method of determining the strength of rocks *in situ*, *Int. J. Rock Mech. Min. Sci.*, *2*, 127–134, doi:10.1016/0148-9062(65)90009-4.

Katz, O., Z. Reches, and J. C. Roegiers (2000), Evaluation of mechanical rock properties using a Schmidt Hammer, *Int. J. Rock Mech. Min. Sci.*, *37*, 723–728, doi:10.1016/S1365-1609(00)00004-6.

Kennedy, B. A. (1976), Valley-side slopes and climate, in *Geomorphology and Climate*, edited by E. Derbyshire, pp. 171–201, John Wiley, New York.

Kirkby, M. J., K. Atkinson, and J. G. Lockwood (1990), Aspect, vegetation cover, and erosion on semi-arid hillslopes, in *Vegetation and Erosion*, edited by J. B. Thornes, pp. 25–39, John Wiley, New York.

Koons, D. (1955), Cliff retreat in the southwestern United States, *Am. J. Sci.*, *253*, 44–52.

Matsuoka, N. (1988), Laboratory experiments on frost shattering of rocks, *Sci. Rep. Inst.Geosci. Univ. Tsukuba Sec. A*, *9*, 1–36.

Matsuoka, N. (1990), The rate of bedrock weathering by frost action: Field measurements and a predictive model, *Earth Surf. Processes Landforms*, *15*, 73–90, doi:10.1002/esp.3290150108.

McAuliffe, J. R., L. Scuderi, and L. D. McFadden (2006), Tree-ring record of hillslope erosion and valley floor dynamics: Landscape responses to climate variation during the last 400 years in the Colorado plateau, north-eastern Arizona, *Global Planet. Change*, *50*, 184–201, doi:10.1016/j.gloplacha.2005.12.003.

McFadden, L. D., and J. R. McAuliffe (1997), Lithologically influenced geomorphic responses to Holocene climatic changes in the Southern Colorado plateau, Arizona: A soil-geomorphic and ecologic perspective, *Geomorphology*, *19*, 303–332, doi:10.1016/S0169-555X(97)00017-2.

McFadden, L. D., and J. C. Tinsley (1985), The rate and depth of accumulation of pedogenic carbonate accumulation in soils: Formulation and testing of a compartment model, in *Soils and Quaternary Geology of the Southwestern United States*, *Geol. Soc. Am. Spec. Pap.*, vol. 203, edited by D. L. Weide and M. L. Faber, pp. 23–42, Geol. Soc. Am., Boulder, Colo.

McFadden, L. D., J. Gosse, J. R. McAuliffe, L. Scuderi, G. Meyer, and B. N. Burnett (2005), Determination of hillslope erosion rates during the late Holocene based on cosmogenic surface age dating of hoodoos, north-eastern Arizona, *Geol. Soc. Am. Abstr. Programs*, *37*(7), 232.

McMahon, D. R. (1998), Soil, landscape and vegetation interactions in a small semi-arid drainage basin: Sevilleta National Wildlife Refuge, New Mexico, M.S. thesis, 174 pp., N. M. Inst. of Min. and Technol., Socorro, N. M.

McMahon, D. R., J. B. J. Harrison, J. M. H. Hendrickx, and E. Muldavin (1996), Microclimatic controls on soil formation across opposite-lying hillslopes in a semi-arid drainage basin in central New Mexico, *Geol. Soc. Am. Abstr. Programs*, *28*(7), 111.

Melton, M. A. (1960), Intravalley variation in slope angles related to microclimate and erosional environment, *Geol. Soc. Am. Bull.*, *71*, 133–144, doi:10.1130/0016-7606(1960)71[133:IVISAR]2.0.CO;2.

Mills, H. H. (1981), Boulder deposits and the retreat of mountain slopes, or, "gully gravure" revisited, *J. Geol.*, *89*, 649–660.

Naylor, S., and E. J. Gabet (2007), Valley asymmetry and glacial versus nonglacial erosion in the Bitterroot Range, Montana, USA, *Geology*, *35*, 375–378, doi:10.1130/G23283A.1.

Penck, W. (1924), *Die Morphologishe Analyse: Ein Kapitel der Physicalischen Geologie*, *Geogr. Abh. Reihe*, vol. 2, Engelhorn, Stuttgart, Germany.

Pettijohn, F. J., P. E. Potter, and R. Siever (1973), *Sand and Sandstone*, 553 pp., Springer-Verlag, Berlin.

Phillips, F. M., L. A. Peeters, M. K. Tansey, and S. N. Davis (1986), Paleoclimatic inferences from an isotopic investigation of groundwater in the central San Juan basin, New Mexico, *Quat. Res.*, *26*(2), 179–193, doi:10.1016/0033-5894(86)90103-1.

Schmidt, K. H. (1989), The significance of scarp retreat for Cenozoic land-form evolution on the Colorado plateau, USA, *Earth Surf. Processes Landforms*, *14*, 93–105, doi:10.1002/esp.3290140202.

Schmidt, K. M., J. J. Roering, J. D. Stock, W. E. Dietrich, D. R. Montgomery, and T. Schaub (2001), The variability of root cohesion as an influence on shallow landslide susceptibility in the Oregon Coast Range, *Can. Geotech. J.*, *38*, 995–1024, doi:10.1139/cgj-38-5-995.

Schumm, S. A., and R. J. Chorley (1966), Talus weathering and scarp recession in the Colorado plateaus, *Z. Geomorphol.*, *10*, 11–36.

Selby, M. J. (1980), A rock mass strength classification for geomorphic purposes: With tests from Antarctica and New Zealand, *Z. Geomorphol.*, *24*(1), 31–51.

Selby, M. J. (1982), Controls on the stability and inclinations of hillslopes formed on hard rock, *Earth Surf. Processes Landforms*, *7*, 449–467, doi:10.1002/esp.3290070506.

Selby, M. J. (1993), *Hillslope Materials and Processes*, 480 pp., Oxford Univ. Press, Oxford, UK.

Sjöberg, R., and N. Broadbent (1991), Measurement and calibration of weathering, using the Schmidt hammer, on wave washed moraines on the upper Norrland coast, Sweden, *Earth Surf. Processes Landforms*, *16*, 57–64, doi:10.1002/esp.3290160107.

Small, R. J., and M. J. Clark (1982), *Slopes and Weathering*, 112 pp., Cambridge Univ. Press, Cambridge, UK.

Stokes, S., and C. S. Breed (1993), A chronostratigraphic re-evaluation of the Tusayan Dunes, Moenkopi plateau and southern Ward Terrace, Northeastern Arizona, in *The Dynamics and Environmental Context of Aeolian Sedimentary Systems, Geol. Soc. Am. Spec. Publ.*, vol. 72, edited by K. Pye, pp. 75–90, Geol. Soc. Am., Boulder, Colo.

Stute, M., J. F. Clark, P. Schlosser, and W. S. Broecker (1995), A 30,000 yr continental paleotemperature record derived from noble gasses dissolved in groundwater from the San Juan basin, New Mexico, *Quat. Res.*, *43*, 209–220, doi:10.1006/qres.1995.1021.

Thornthwaite, C. W. (1961), The task ahead, *Ann. Assoc. Am. Geogr.*, *51*, 345–356, doi:10.1111/j.1467-8306.1961.tb00385.x.

Tillery, A., P. Fawcett, L. McFadden, L. Scuderi, and J. McAuliffe (2003), Late Holocene behavior of small drainage basins on the Colorado plateau: Influences of lithology, basin form, and climate change, in *Geology of the Zuni Plateau*, edited by S. Lucas et al., pp. 197–207, N. M. Geol. Soc., Socorro, N. M.

Tillery, A. C. (2003), Late Holocene behavior of small basins on the Colorado plateau near Blue Gap, Arizona: Lithologic, morphometric and climatic influences, M.S. thesis, 173 pp., Univ. of N. M., Albuquerque, N. M.

Twidale, C. R., and E. M. Campbell (1986), Localized inversion on steep hillslopes: Gully gravure in weak and resistant rocks, *Z. Geomorphol.*, *30*, 35–46.

Vicente, M. A. (1983), Clay mineralogy as the key factor in weathering of ''Arenisca dorada'' (Golden Sandstone) of Salamanca, Spain, *Clay Miner.*, *18*, 215–217, doi:10.1180/claymin.1983.018.2.11.

Wahrhaftig, C. (1965), Stepped topography of the southern Sierra Nevada, California, *Geol. Soc. Am. Bull.*, *76*, 1165–1190, doi:10.1130/0016-7606(1965)76[1165:STOTSS]2.0.CO;2.

Walder, J., and B. Hallet (1985), A theoretical model of the fracture of rock during freezing, *Geol. Soc. Am. Bull.*, *96*, 336–346, doi:10.1130/0016-7606(1985)96<336:ATMOTF>2.0.CO;2.

Wawrzyniec, T. F., L. D. McFadden, A. Ellwein, G. A. Meyer, L. Scuderi, J. McAuliffe, and P. Fawcett (2007), Chronotopographic analysis directly from point cloud data: A method for detecting small, seasonal hillslope change, Black Mesa escarpment, NE Arizona, *Geosphere*, *3*, 550–567, doi:10.1130/GES00110.1.

Webster, S. L., R. H. Grau, and T. P. Williams (1992), *Description and Application of Dual Mass Dynamic Cone* Penetrometer, U.S. Army Corps of Eng., Vicksburg, Miss.

Wells, S. G., L. D. McFadden, and J. D. Schultz (1990), Eolian landscape evolution and soil formation in the Chaco dune field, southern Colorado plateau, New Mexico, *Geomorphology*, *3*, 517–546, doi:10.1016/0169-555X(90)90019-M.

Wilson, L. (1968), Asymmetric valleys, in *The Encyclopedia of Geomorphology*, edited by R. W. Fairbridge, pp. 30–33, Reinhold, New York.

Zhu, C., R. K. Waddell, I. Star, and M. Ostrander (1998), Responses of ground water in the Black Mesa basin, northeastern Arizona, to paleoclimatic changes during the late Pleistocene and Holocene, *Geology*, *26*, 127–130, doi:10.1130/0091-7613(1998)026<0127:ROGWIT>2.3.CO;2.

———————————

B. N. Burnett, L. D. McFadden, and G. A. Meyer, Department of Earth and Planetary Sciences, University of New Mexico, Albuquerque, NM 87131, USA. (burnettben@yahoo.com; lmcfadnm@unm.edu; gmeyer@unm.edu)